High Temperature Oxidation of Single Carbon Nanoparticles: Dependence on Surface Structure, and Probing Real-Time Structural Evolution via Kinetics.

Daniel J. Rodriguez[1], Chris Y. Lau[1], Abigail M. Friese[1], Alexandre Magasinski[2], Gleb Yushin[2], and Scott L. Anderson[1]*

[1]Department of Chemistry, University of Utah, 315 S. 1400 E., Salt Lake City, UT 84112
[2]School of Materials Science and Engineering, Georgia Institute of Technology, 771 Ferst Dr. NW, Atlanta, GA 30322

ABSTRACT: O_2-oxidation and sublimation kinetics for >30 individual nanoparticles (NPs) of five different feedstocks (graphite, graphene oxide, carbon black, diamond, and nano-onion) were measured using single nanoparticle mass spectrometry at temperatures (T_{NP}) in 1100 – 2900 K range. It was found that oxidation, studied in the 1200 to 1600 K range, is highly sensitive to NP surface structure, with etching efficiencies (EE_{O2}) varying by up to four orders of magnitude, whereas sublimation rates, significant only for $T_{NP} \geq$ ~1700 K, varied by only a factor of ~3. Its sensitivity to NP surface structure makes O_2 etching a good real-time structure probe, which was used to follow evolution of the NP surface structures over time as they were either etched or annealed at high T_{NP}. All types of carbon NPs were found to have initial EE_{O2} values in the range near 10^{-3} Da/O_2 collision, and all eventually evolved to become essentially inert to O_2 ($EE_{O2} < 10^{-6}$ Da/O_2 collision), however, the dependence of EE_{O2} on time and mass loss was very different for NPs from different feedstocks. For example, diamond NPs evolved rapidly and monotonically toward inertness, and evolution occurred in both oxidizing and inert atmospheres. In contrast, graphite NPs evolved only under oxidizing conditions, and etched with complex time dependence, with multiple waves of fast-but-non-monotonic etching, separated by periods of near-inertness. Possible mechanisms to account for the complex etching behavior are proposed.

1. Introduction

Oxidation of carbon nanoparticles (NPs) at high temperatures is relevant to many applications of carbon nano-materials, but there are also interesting fundamental questions relating reactivity to NP surface structure, which can vary dramatically for different carbon materials (graphitic, diamond, fullerene, etc.).[1-2] Even for a particular type of carbon NP, there can be large NP-to-NP variations in the number and types of exposed surface sites, strongly affecting the rates of processes such as sublimation or oxidation.[3] Finally, even for a *single* NP, the surface structure may evolve during reaction, resulting in large rate variations. To enable study of these effects, we have developed an approach to measuring surface reaction kinetics for individual NPs, held in an electrodynamic trap.[4-5]

For example, we previously found that sublimation of graphitic NPs at temperatures (T_{NP}) > 1700 K was substantially faster than the rates for bulk graphite,[6-8] varied by up to an order of magnitude from NP-to-NP, and slowed significantly over time, correlated with increases in optical emissivity. This behavior was attributed to the NPs initially having large, but highly variable numbers of under-coordinated surface sites, and that preferential sublimation at such sites reduces the numbers of such sites over time, reducing the rates, and modifying the optical properties.[4]

We also reported a study of O_2 oxidation of graphitic NPs.[5] Etching rates peaked in the 1200 – 1500 K range, dropping at higher T_{NP}. Etching rates varied substantially from NP-to-NP and fluctuated over time for individual NPs. Both effects were attributed to variations in the numbers of under-coordinated reactive sites on the NP surfaces, which evolved as the NPs etched. Surprisingly, it was also found that graphitic NPs eventually evolved to be essentially inert to O_2 in the 1200 to 1900 K range, implying that the number of exposed reactive sites dropped to near zero. It was speculated that his evolution to O_2 inertness resulted from a transformation of at least the surface layer, to "nano-onion" (multi-wall fullerene) structure.

This interpretation of the previous results, as well as results presented below, relies on extensive literature on oxidation of various forms of carbon, particularly graphite, some of which is discussed in the SI. Briefly, etching is O_2 dissociative adsorption, followed by CO/CO_2 desorption, and the decrease at higher T_{NP} has been attributed to competition from O-atom desorption.[9-10] Surface chemistry studies have shown that perfect graphite basal planes have near-zero reactivity towards O_2 in this temperature range,[11-12] but etching is observed at sputter-induced basal plane defects[13-17] and at prismatic surfaces,[18] which expose basal plane edges. For example, Olander *et al.*[11] observed etching at sputtered basal plane defects from 1400 – 1500 K at O_2 fluxes of ~100 O_2 collision/sec/nm^2, about 30% lower than our flux. Etching at defects tends to expand the defects laterally, leading to 2D etch pit formation.[13-17] For example, Edel *et al.*[17] studied pit formation during HOPG etching to peak at 1200 – 1400 K, using O_2 fluxes of ~0.1 O_2 collisions/sec/nm^2. It is interesting to note that the T_{NP} range where we observe the maximum etching rates is similar to the range seen in the surface chemistry experiments, but also in experiments with bulk graphite at much higher pressures. For example, Wall *et al.*[19] observed the steady state etching rates for bulk graphite to peak between 1700 – 1900 K, and Rosner *et al.*[20] observed peaks in the 1500 to 1750 K range, with O_2 partial

pressures in the Torr range, compared to the ~4 x 10^{-5} Torr pressures typical of our experiments.

The study reported here had two objectives. We measured the variations in initial O_2 reactivity for different NP feedstocks (graphite, graphene oxide, carbon black, diamond, and nano-onions[21]), and also the variations between individual NPs for each carbon material. Then, we studied the structural evolution over time for each type of carbon NP, exploiting the high sensitivity of the O_2 etching rates on NP surface structure.

2. Results

Our experimental protocols for single NP kinetics measurements have been reported previously[4-5] along with the method for T_{NP} determination, and analysis of the uncertainties in NP mass and reaction rates (~1.3% absolute, ~0.2% relative) and T_{NP} (~6.2% absolute, ~2% relative). Further details are given in the SI. Briefly, a single carbon NP is trapped in a 3D quadrupole[22] and laser heated above 1000 K, allowing the NP mass (M) and charge (Q) to be monitored over time, with temperature (T_{NP}) determined from the NP emission spectrum (**Fig. S1**).[23-24] Monitoring M vs. time for an NP held in argon buffer gas (2 mTorr) allows the baseline mass loss rate (R_{base}) to be measured. For $T_{NP} \geq 1600$ K, R_{base} is dominated by sublimation ($R_{sublimation}$), but at lower T_{NP} there can be noticeable mass loss from reactions with background gasses (e.g. O_2, H_2O) in the vacuum system. To measure oxidation kinetics, a partial pressure of O_2 (P_{O2}) is added to the argon, resulting in a new mass loss rate, which is converted to the oxidative etching rate (R_{oxid}) by subtracting R_{base} measured before and after each oxidation period. To allow comparisons between different size NPs, R_{base}, $R_{sublimation}$, and R_{oxid} are expressed in terms of Da/sec/nm^2, i.e., the mass loss rates are normalized to nominal NP surface areas, which are calculated from the NP mass assuming spherical shape and the bulk density of the NP material. In most cases, the R_{oxid} values are further converted to etching efficiencies (EE_{O2}), i.e., the mass loss *per* O_2 collision (Da/O_2 collision), using collision rates calculated from P_{O2} and the nominal NP surface area. Because the nominal surface areas are lower limits on the true surface areas, the rates and EE_{O2} values are upper limits.

2.1 – Kinetics for a Graphite NP and a Diamond NP

Fig. 1 shows examples of simple O_2 oxidation experiments for both a graphite NP and a diamond NP. Identical experiments for graphene oxide, carbon black, and nano-onion NPs are shown in **Figs. S2** – **S4**. Consider the graphite NP experiment in **Fig. 1A**, where the initial mass was ~39.0 MDa (~37.9 nm diameter for a spherical NP with bulk graphite density (~2.265 g/cm^3) [25]). T_{NP} was initially ramped to 1900 K over a few minutes, then held for ~10 minutes. As the NP was initially heated, contaminants such as methanol or ammonium acetate from the electrospray ionization solution, as well as surface complexes of heteroatoms like O, H, and N, would have desorbed.[26-29] In addition, when NPs are first heated to high T_{NP}, thermionic electron emission occurs, increasing Q to a new steady-state value. Once T_{NP} had stabilized at 1900 K, the slope of M vs. time was used to determine the raw mass loss rate, -1773 Da/sec. Sublimation dominates the mass loss at 1900 K,[4] and while we have no information about the product species, for bulk graphite a distribution of small C_n species is observed.[30-33] The nominal (spherical) surface area of this NP was ~4463 nm^2, giving $R_{sublimation}$ of ~0.4 Da/sec/nm^2, and the total mass sublimed was ~1.4 MDa – roughly a monolayer's (ML's) worth of carbon for a spherical NP of this mass.

Next, T_{NP} was dropped to 1300 K (purple background) to allow Q to be measured (+71e) using the Q-stepping process illustrated in **Fig. S5**, and then T_{NP} was set to 1500 K. R_{base} was near zero (~constant mass) because 1500 K is well below the range where graphite sublimation is significant.[4] At the ~1.39 hour point, 4.3 x

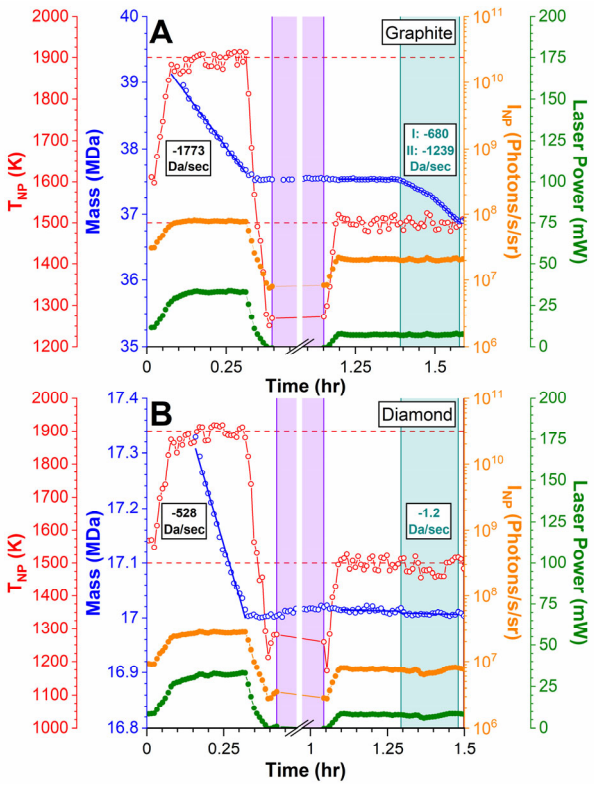

Figure 1. The sublimation and oxidation kinetics for two NPs. Purple-shaded background indicates time intervals when Q-stepping was used to measure Q. Cyan-shaded background indicates periods of O_2 oxidation, and unshaded background indicate periods when only Ar was added to the trap. A). A single graphite NP, first measuring $R_{sublimation}$ at 1900 K and then R_{oxid} at 1500 K with P_{O2} = 4.3 x 10^{-5} Torr. B). An identical experiment, but analyzing a diamond NP.

10^{-5} Torr of O_2 was added (cyan background), resulting in a significant mass loss rate, attributed to etching reactions in which CO (and possibly CO_2) desorb. The raw etching rate accelerated during the ~10 minute oxidation period, from -680 Da/sec to -1239 Da/sec after a few minutes, corresponding to an EE_{O2} of ~1.44 x 10^{-3} Da/O_2 collision, averaged over the oxidation period. A total of ~0.6 MDa was oxidized away, corresponding to ~0.5 ML for a spherical NP.

Fig. 1A also plots the emission intensity, I_{NP} (photons/second/sr, integrated between 600 – 1600 nm) and the laser power (mW) required to heat the NP to the T_{NP} setpoint values. In this example, both were nearly constant during each constant T_{NP} period, indicating that NP optical properties (near-IR emissivity and 532 nm absorptivity) were not significantly altered by the heating and modest mass loss in this experiment.

T_{NP} is determined by the balance between various heating and cooling processes, and it should be noted that for the relatively slow mass loss rates studied here, the effects of exothermic or endothermic reactions are neglible. For example, a 50 nm diameter NP at 1500 K would radiate ~2 x 10^8 eV/sec, assuming an emissivity of ~0.02, which is reasonable for a sub-wavelength black carbon NP. In addition, collisions with the 300 K Ar buffer gas would remove an additional ~7 x 10^6 eV/sec, thus laser heating of ~2.07 x 10^8 eV/sec would be required to maintain T_{NP}. Sublimation and oxidation reactions require or produce, at most, a

few eV *per* carbon atom removed, thus even for mass loss rates well above the range studied here, the contributions to heating and cooling are negligible.

The 1500 K EE_{O2} values for the graphene oxide, carbon black, and carbon nano-onion NPs in **Figs. S2 – S4** were all in the same range as that for the graphite NP in **Fig. 1**: 1.0 x 10^{-3}, ~7 x 10^{-4}, and 1.5 x 10^{-3} Da/O_2 collision, respectively. The factor of ~two variation in EE_{O2} reflects differences in the numbers of reactive sites on the NP surfaces, which are expected to vary due to the distributions of shape and surface structure in the NP feedstocks. **Fig. S6** shows two other experiments of this type, for different graphene oxide and nano-onion NPs. These also showed similar 1900 K sublimation kinetics, but the subsequent oxidation kinetics were more complex, with order-of-magnitude fluctuations in the oxidative mass loss rates (raw rate numbers given in the insets). As discussed previously for graphitic NPs,[5] unsteady oxidation behavior is attributed to evolution of the NP surface site distributions as the surface is etched away, removing and exposing reactive surface sites. More dramatic examples are presented below.

Fig. 1B shows an essentially identical experiment on a diamond NP, but with a very different result. The NP had an initial mass of ~17.3 MDa, which, as discussed in the SI, almost certainly indicates that the NP was an aggregate of smaller (~1 MDa) nanodiamonds. The 1900 K sublimation rate was reasonably constant at -528 Da/sec, corresponding to $R_{sublimation} \approx 0.27$ $Da/sec/nm^2$. The $R_{sublimation}$ values for the six carbon NPs of five different feedstocks (**Figs. 1A**, **S2-S4**, and **S6**) varied by only a factor of ~two, and all fall within the range observed previously for 1900 K sublimation of 20 different graphitic NPs.[4]

In contrast, the 1500 K oxidative etching rate for the diamond NP was far slower than the etching rates for any of the other carbon NPs, as shown by the tiny change in the slope of M vs. time when the diamond NP was exposed to O_2 (cyan background). The (R_{base}-corrected) EE_{O2} value was only ~4 x 10^{-6} Da/O_2 collision, i.e., orders of magnitude smaller than the EE_{O2} values for the graphite, graphene oxide, carbon black, and nano-onion NPs under identical conditions (**Figs. 1A**, **S2-S4**, and **S6**). These data, therefore, raise two questions: 1. Why the diamond NP was so unreactive compared to all the other carbon NPs. 2. Why the 1900 K $R_{sublimation}$ values were so similar for all the NPs, including the diamond NP which was nearly inert to O_2.

Both oxidation and sublimation are expected to be sensitive to the NP surface structure. For graphitic or other black-carbon NPs, we expect that fully-coordinated sp^2 sites should be unreactive toward O_2,[11-12] but under-coordinated carbon at exposed basal plane edges or defects should be reactive.[13-18, 34-36] Unreconstructed diamond surfaces also have many under-coordinated atoms, but various reconstructions are possible,[37-38] thus the negligible reactivity observed in **Fig. 1B** could be taken as evidence that nanodiamonds are inherently O_2-resistant at 1500 K, or that the diamond NP had already evolved to an O_2-resistant surface structure during the 1900 K sublimation period. The 1900 K sublimation rates in **Fig. 1** (0.4 $Da/sec/nm^2$ for graphite; 0.27 $Da/sec/nm^2$ for diamond) correspond to desorption of ≤ 1% of the surface atoms/second. Thus, while sublimation is still rather slow at 1900 K, and thus should be dominated by under-coordinated sites with low C_n desorption energies, 1500 K oxidation is clearly far more sensitive to surface structure, and therefore is a superior probe for the presence of reactive sites on NP surfaces.

2.2 – T_{NP} Dependence and Diamond NP Reactivity

Fig. 2A examines the effects of time and T_{NP} on the O_2 reactivity of a single diamond NP. Prior to the start of the data record shown, the NP had been trapped and Q-stepped, but T_{NP} was kept below

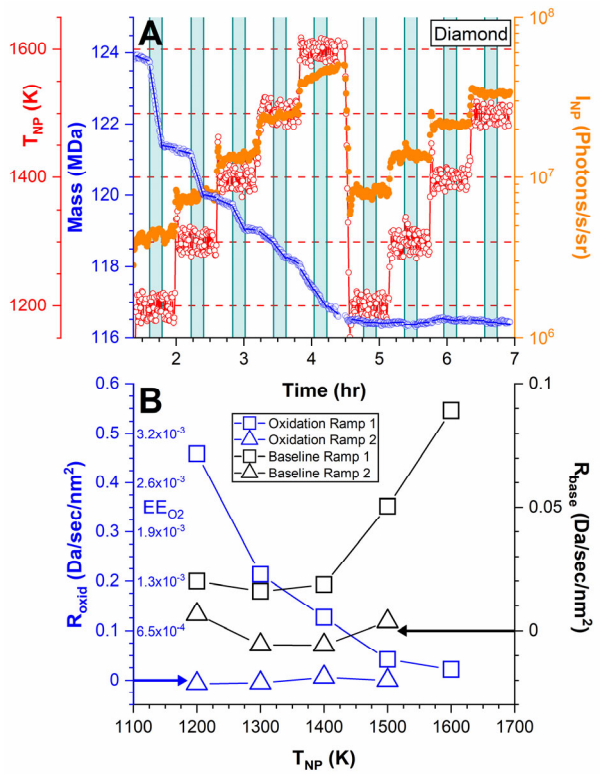

Figure 2. A). A diamond NP (M = 123.9 MDa) is T_{NP} ramped twice measuring R_{oxid} and R_{base}. B). R_{base} (black, right axis) and R_{oxid} and EE_{O2} (blue, left axis with dual scales) plotted vs. T_{NP} for the two heat ramps.

1200 K to minimize thermal effects on the NP prior to the oxidation measurements. T_{NP} was then stepped from 1200 to 1600 K, dropped back to 1200 K, then stepped again to 1500 K. At each T_{NP}, R_{base} was measured before and after each oxidation period (cyan background, P_{O2} = 4.3 x 10^{-5} Torr). **Fig. 2B** plots the R_{base}, R_{oxid}, and EE_{O2} values for each T_{NP}.

As T_{NP} was initially stepped to 1400 K, R_{base} was constant at ~0.02 $Da/sec/nm^2$, due to background O_2 and H_2O reactions, then increased rapidly for $T_{NP} \geq$ 1500 K, signaling the onset of sublimation. When O_2 was added, the mass loss rates increased substantially ($R_{oxid} \gg R_{base}$) for low T_{NP}, but with increasing T_{NP} the effect of O_2 addition decreased, becoming negligible at 1600 K ($R_{oxid} \approx$ zero). Then, during the 2nd ramp, the mass losses in both Ar and O_2 were essentially zero, i.e., the NP had changed irreversibly during the first T_{NP} ramp, substantially reducing both the sublimation and oxidation rates.

The initial diamond NP reactivity at 1200 K was high and constant over the first ~10 minute oxidation period, even though ~2.25 MDa was etched away, and the 1200 K EE_{O2} value was ~3 x 10^{-3} Da/O_2 collision, which is two to five times *greater* than the 1500 K EE_{O2} values for the black carbon NPs in **Figs. 1A** and **S2-S4**. We previously measured 1200 K R_{oxid} values for a number of graphitic NPs,[5] and the corresponding EE_{O2} values averaged ~1.7 x 10^{-2} Da/O_2 collision, i.e., the 1200 K reactivity for this diamond NP was lower than the average for graphite at 1200 K, but only by a factor of ~6. As T_{NP} was stepped to 1600 K, however, the diamond NP EE_{O2} dropped to near zero by 1600 K, and remained near zero in the 2nd ramp, indicating that a drastic, irreversible decrease in the number of under-coordinated reactive surface sites occurred as the NP was initially heated to 1600 K, losing 7.5 MDa of mass (nominally ~3 ML's worth).

Heating/etching also caused irreversible changes in NP optical properties, as shown by the higher I_{NP} values seen during the 2nd ramp, compared to the 1st (note log scale). For example, at 1200 K, I_{NP} averaged ~4 x 10^7 during the 1st ramp but doubled to ~8 x 10^7 during the 2nd, with only a small change in the spectral shape (**Fig. S7**). The evolution is also shown by the increase in I_{NP} during the higher T_{NP} steps in the 1st ramp. Irreversible emission brightening caused by NP heating was also observed for graphitic NPs,[4-5, 24] and those studies also noted the apparent correlation between emission brightening and decreasing rates of sublimation and oxidation, which was interpreted as suggesting a inverse correlation between brightness and numbers of under-coordinated surface sites.

Figs. 1 and **2** show that diamond NPs are quite reactive at 1200 K, and that reactivity decreases irreversibly under both inert and oxidative conditions at higher T_{NP}. **Fig. 3** shows an experiment to test how a diamond NP evolves under inert conditions, using O_2 oxidation as a probe of changes in the number of exposed reactive sites. An NP of initial mass ~46.5 MDa was trapped and Q-stepped (purple background), carefully keeping T_{NP} below 1150 K to minimize changes to the NP. T_{NP} was then set to 1200 K, and the mass loss rates were measured in both argon and with 4.3 x 10^{-5} Torr of O_2 added (cyan background) to characterize the initial reactivity. After a brief oxidation period, the NP was subjected to two stepwise T_{NP} ramps from 1200 – 2000 K under inert conditions, and then a second 1200 K oxidation period was used to probe changes in the reactivity.

The initial 1200 K EE_{O2} was ~1.2 x 10^{-3} Da/O_2 collision, i.e., lower, but in the same range as the initial 1200 K EE_{O2} for the diamond NP in **Fig. 2**, presumably reflecting the NP-to-NP variations in shape and surface structure. Note that the mass loss rate slowed significantly during the 10 minute initial oxidation period (curvature in M vs. time), such that the average EE_{O2} was only ~6.1 x 10^{-4} Da/O_2 collision. After two T_{NP} ramps, EE_{O2} during the 2nd oxidation period was zero within our sensitivity – at least 250 times less reactive.

As the NP was first heated, a non-zero R_{base} was observed between 1400 and 1700 K (**Fig. 3B**), attributed to etching reactions with background gasses. In the 1800 – 2000 K range, R_{base} increased rapidly, due to increasing rates for sublimation, with $R_{sublimation}$ values similar to those previously observed for graphitic NPs.[4] During the 2nd ramp, R_{base} was zero up to 1700 K, indicating that the NP had already become inert to etching, but the rapid onset of mass loss at 1800 K showed that sublimation was still fast at high T_{NP}. $R_{sublimation}$ at 2000 K during the 2nd ramp was only ~36% slower than in the 1st. The results show that the NP evolved drastically during the 1st ramp as ~3 MDa (~2 ML) sublimed.

2.3 – Can Reactivity of "Evolved" Carbon NPs be Restored?

Fig. 3 shows that even after the diamond NP had become inert to O_2, its sublimation rate was still substantial, and one obvious question is whether it might be possible to restore O_2 reactivity by rapidly subliming material from the NP surface during a short period at high T_{NP}. A test of this idea is shown in **Fig. 3C**, which continues the time record from **Fig. 3A**, when at the point just before the 2nd oxidation period showing that the NP had already become O_2 inert. The NP was then held in argon with one laser holding T_{NP} = 1200 K, while a second laser (10 W, duty-factor modulated CO_2 laser) was used to flash heat the NP for three short periods (solid T_{NP} points). To avoid vaporizing the NP in the first flash, the CO_2 laser power was increased between each flash until a large mass loss was observed. The SI gives details of the process used to estimate the T_{NP} during each CO_2 flash (**Fig. S8**).

The 1st flash increased T_{NP} to ~2350 K for three seconds, resulting in sublimation of only ~37 kDa (less than the width of the

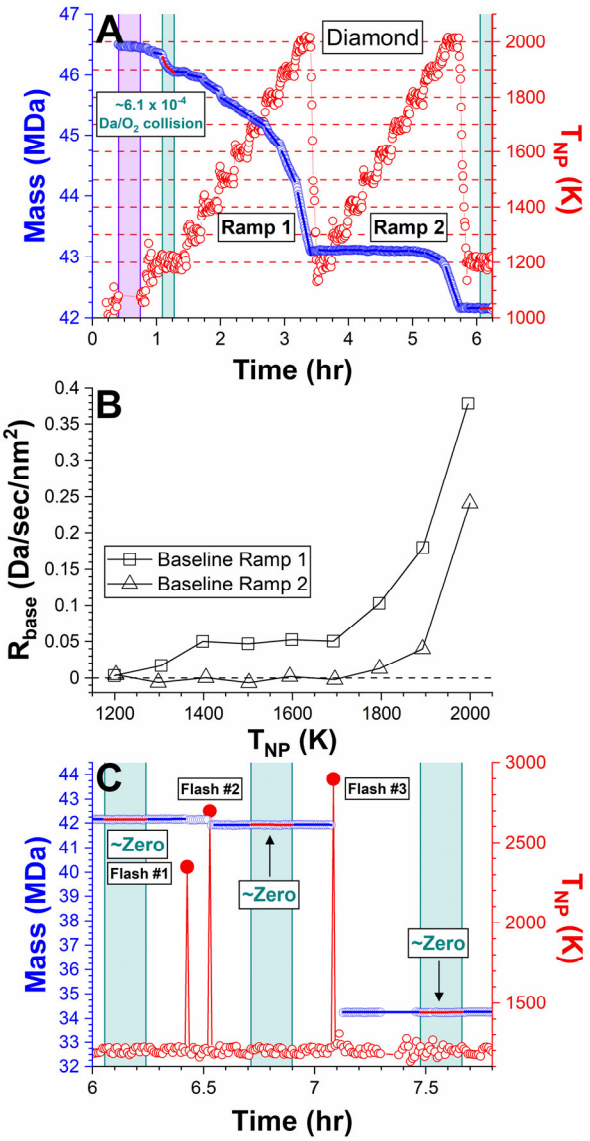

Figure 3. A). A ~46.5 diamond NP was T_{NP} stepped twice from 1200 – 2000 K. EE_{O2} was measured before and after. B). R_{base} vs. T_{NP} for the two heat ramps in frame A. C). The NP was flashed to high T_{NP} to see if R_{oxid} could be restored.

mass points), therefore a second flash to $T_{NP} \approx 2700$ K was applied, causing sublimation of ~216 kDa over two seconds. When O_2 was added to probe reactivity, there was no significant mass loss, i.e., the NP remained inert. After switching off the O_2 flow, the NP was flashed to ~2900 K for 12 seconds, causing a much larger mass loss of ~7.7 MDa accompanied by a 6e *decrease* in the NP charge. As noted in the discussion of **Figs. 1** and **S5**, NPs often undergo thermionic electron emission, especially when first heated to higher temperatures, however, this *increases* Q in increments of +e, giving rise to well defined steps in secular frequency (**Fig. S5**). The simultaneous decrease in M and Q observed during flash heating of the diamond NP, is attributed to loss of positively charged fragments from the NP. In this case, where the NP was clearly a large aggregate of primary nanodiamonds, fragmentation may have involved loss of individual nanodiamonds or small aggregates. Given that the estimated T_{NP} during the flash was high, rapid

sublimation also must have occurred, and it is not possible to separate the mass losses due to fragmentation and sublimation.

It should be noted that fragmentation was not observed in the other experiments, presumably because the T_{NP} ranges, and resulting sublimation or etching rates, were more modest. If fragmentation had occurred, it would have been obvious as secular frequency steps that did not match the step size expected for electron emission. The absence of such events, even for aggregate NPs, suggests that aggregates must be reasonably strongly bound, such that they break up only under conditions of rapid sublimation or etching.

Despite this major disruption of the NP surface in **Fig. 3C**, the NP remained inert to O_2 after re-cooling to 1200 K. In this experiment, flash heating and subsequent cooling was done in argon, with O_2 reactivity probed after a period of 1200 K storage in argon. To test the possibility that an inert NP might briefly become O_2-reactive after a heating flash, a similar experiment was done in which the NP was held under oxidizing conditions during the flash heating/cooling periods (**Fig. S9**). This experiment also found no evidence of restoration of O_2 reactivity, even though there was several ML's worth of material sublimed during the highest T_{NP} flash.

2.4 – Effects of O_2 on Carbon NPs at Constant T_{NP} and P_{O2}

To more clearly separate the effects of time and T_{NP} on NP evolution, a series of experiments were done in which NPs were allowed to evolve over time under constant reaction conditions. An example is shown in **Fig. 4**, for a carbon black NP with initial mass of ~59.9 MDa, which if spherical with the bulk density (~1.8 g/cm^3) [39] would have diameter of ~47.3 nm. Before the start of the data shown, the NP had been heated to 1900 K for 10 minutes for cleaning, then at the beginning of the data record, it was being held at 1300 K for Q-stepping (purple background). T_{NP} was then set to 1500 K, and held for > 8 hours. R_{base} was measured (unshaded background), then P_{O2} was set to 4.3 x 10^{-5} Torr for the rest of the experiment (cyan background). The M vs. time record was divided into periods with near-constant mass loss rates, and fit to obtain the average slopes during each period. Periods with slopes greater than the initial R_{base} are indicated by red fit lines and roman numeral labels. Periods with slopes near R_{base} (i.e., $R_{oxid} \approx$ zero) are shown with blue regression lines without labels. **Fig. 4B** shows how the EE_{O2} values varied as the NP lost mass, using the same colors and labels as in frame A. The blue points with downward arrows indicate time periods when the slope of M vs. time $\approx R_{base}$, corresponding to R_{oxid} and $EE_{O2} \approx$ zero. From our ability to detect small slope differences, we roughly estimate that our sensitivity limit for EE_{O2} is ~10^{-6} Da/O_2 collision.

EE_{O2} was initially 1.4 x 10^{-3} Da/O_2 collision – comparable to the values for the black carbon NPs in **Figs. 1A**, **S2-S4**, and **S6**. Etching gradually slowed over the first ~4 hours (II – VI) as the NP lost ~4 MDa, dropping below 10^{-6} Da/O_2 collision just before the 5 hour mark. EE_{O2} remained <10^{-6} for ~45 minutes, followed by two additional waves of etching, during which EE_{O2} abruptly increased by nearly three orders of magnitude then gradually dropped back below 10^{-6} with 1 to 1.5 MDa of mass lost in each wave. The experiment was terminated at 10 hours after a 1.25 hour period with insignificant mass loss. In total, the NP lost ~12% of its initial mass. For reference, a spherical carbon black NP with mass in this range would have ~3% of its mass (~1.7 MDa) in the surface monolayer, thus the mass losses during the 1st, 2nd, and 3rd etching waves correspond to ~2.4, ~0.6, and ~0.9 ML's worth of material. **Fig. S10** shows a similar experiment for a larger carbon black NP (104.5 MDa) at 1500 K, with P_{O2} = 2.1 x 10^{-5} Torr. The results for all NPs are aggregated and discussed below, but in brief, the initial EE_{O2} (1.8 x 10^{-3} Da/O_2 collision) and evolution behavior were

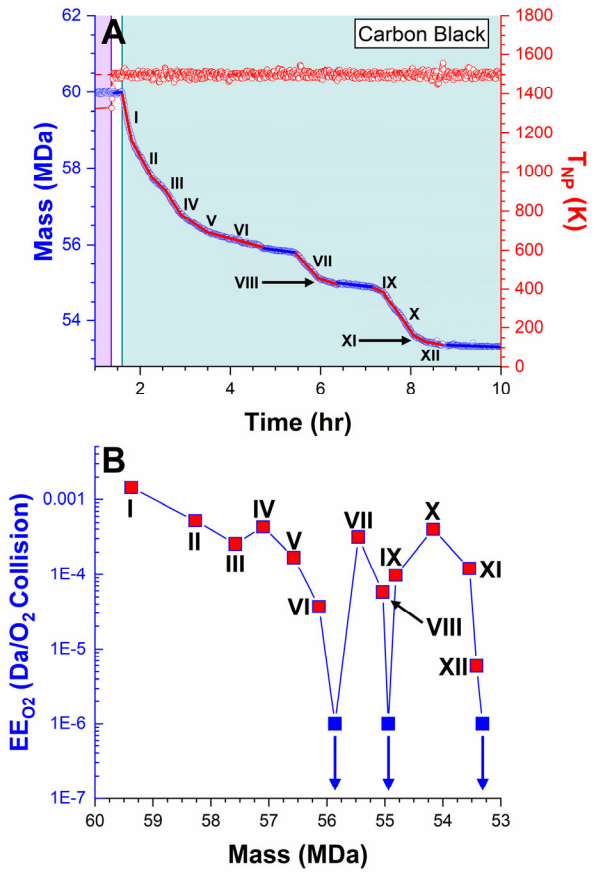

Figure 4. A). A carbon black NP at constant T_{NP} and P_{O2}. B). EE_{O2} vs. mass is plotted. Roman numerals allow for comparison between frames A and B.

similar to those for the carbon black NP in **Fig. 4**, except that oscillations in EE_{O2} were weaker (~1 order of magnitude).

Fig. 5 shows the evolution of a graphene oxide NP under conditions identical to those in **Fig. 4**, and also plotted identically. The NP was briefly heated to 1900 K, which should be sufficient to desorb all the oxygen surface functional groups,[26-28] leaving a highly defective graphene NP (i.e., reduced graphene oxide), with mass of ~37.6 MDa. T_{NP} was held at 1500 K for a total of 22 hours, the first 16 of which are shown. After measuring R_{base} in argon, 4.3 x 10^{-5} Torr of O_2 was added (cyan background), leading to rapid etching (EE_{O2} ~1.1 x 10^{-3} Da/O_2 collision) that continued at near-constant rate (I - IX) for ~3 hours as the NP lost ~16% of its initial mass. At that point, the mass loss slowed abruptly but continued for the next 12 hours at an average rate near 10^{-4} Da/O_2 collision, but with significant oscillations, including two periods with EE_{O2} < 10^{-6}. At ~16 hours, EE_{O2} dropped below 10^{-6} Da/O_2 collision and remained there until the experiment was terminated at the ~22 hour mark. The total mass lost was ~20%, most of which occurred during the initial ~3 hours.

We previously reported similar experiments for graphite and graphene NPs,[5] but at different T_{NP} and/or P_{O2} values, therefore to facilitate comparisons with other carbon NPs, new graphite NP experiments were done under conditions identical to those in **Figs. 4** and **5**, one of which is shown in **Fig. 6**. Because the kinetics were so complex, different fit line and symbol colors have been used instead of Roman numerals to help associate the M vs. time data in **Fig. 6A** with the EE_{O2} vs. M data in **Fig. 6B**. The 36 MDa initial mass NP was first flashed to 1900 K (losing ~1 MDa at $R_{sublimation}$

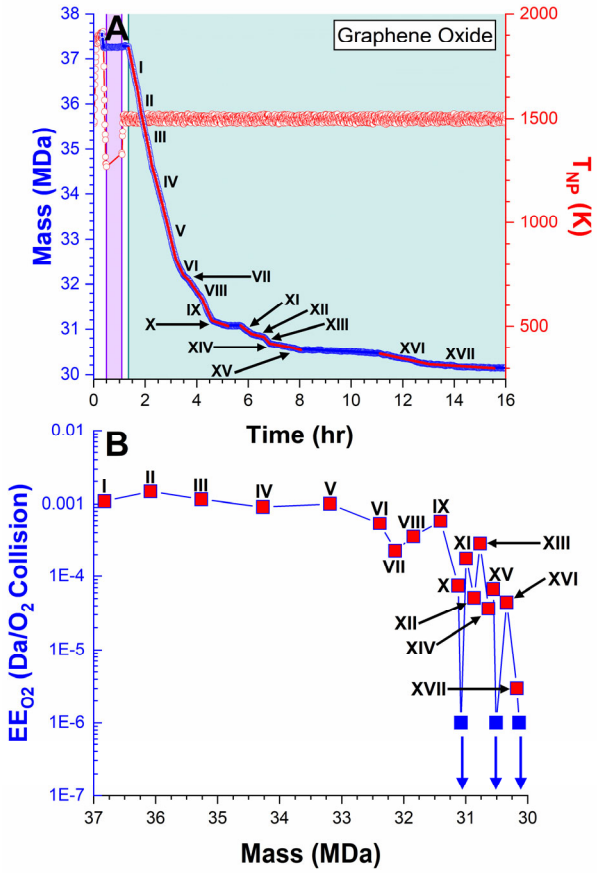

Figure 5. A). A graphene oxide NP at constant T_{NP} and P_{O2}. B). EE_{O2} vs. mass shows the decrease in reactivity.

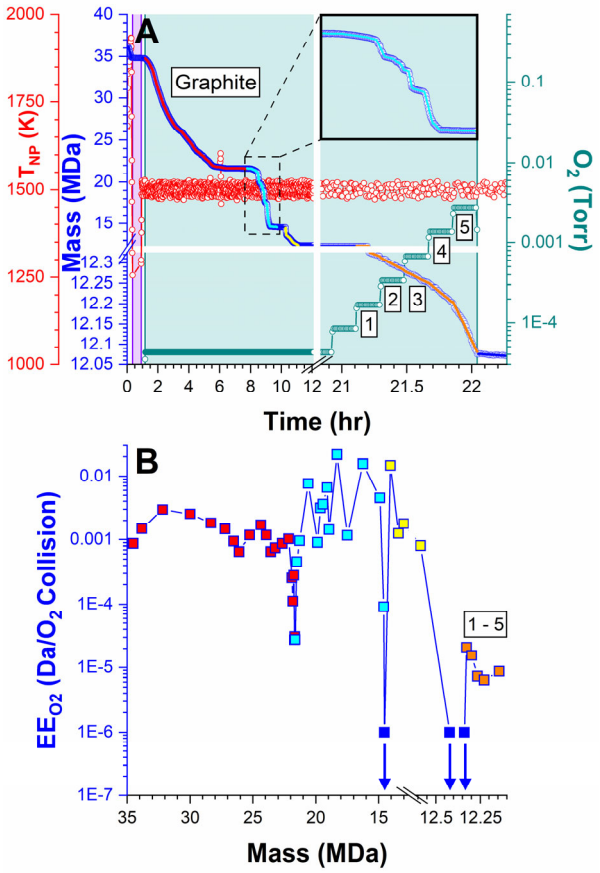

Figure 6. A). A graphite NP at constant T_{NP} and P_{O2}. B). EE_{O2} vs. mass is plotted, and the NP loses ~64% of its mass before becoming inert.

= 0.45 Da/sec/nm^2), cooled to <1300 K for Q-stepping, then held at 1500 K for the rest of the experiment. After measuring R_{base} at 1500 K (6.4 x 10^{-3} Da/sec/nm^2), 4.3 x 10^{-5} Torr of O_2 was added, resulting in a first wave of fast oxidative mass loss (red fit lines and symbols) that did not end until M had decreased by ~37%. EE_{O2} was initially ~8.8 x 10^{-4} Da/O_2 collision, but increased by a factor of ~4 as M decreased by ~10%, then slowly dropped back to near the initial value over a 4 hour period, with minor (~3x) oscillations. This first wave ended at ~6 hours when EE_{O2} dropped by a factor of ~30, with M remaining near ~22 MDa for ~3 hours. Similar behavior was seen for graphite NPs previously,[5] but we allowed this experiment to continue, resulting in two additional etching waves (cyan and yellow lines and symbols) each lasting about an hour. The carbon black and graphene oxide NPs in **Figs. 4** and **5** also had additional etching waves, however, for graphite, EE_{O2} during the 2nd and 3rd waves reached values up to 25 times higher than the initial EE_{O2}, and in the 2nd wave there were pronounced rate oscillations (see inset). The 2nd and 3rd waves removed ~7 and ~2 MDa, corresponding to ~20% and ~6% of the initial mass, respectively, and the fluctuations during the 2nd wave each removed between 2% and 16% of the NP mass *at the time*, corresponding to ~0.5 to a few MLs' worth of material. The 3rd wave ended at ~11 hours, when EE_{O2} sat below 10^{-6} Da/O_2 collision for more than 10 hours, during which the mass decreased by ~80 kDa, as indicated by the blue points in **Fig. 6B** at ~12.42 and ~12.34 MDa. At this point, the NP had lost ~66% of its initial mass.

Finally, we tested to see if oxidation activity might be restored by increasing P_{O2}, starting at 20 hours (orange regression lines and symbols - note change in mass scale). Doubling P_{O2} had essentially no effect on mass loss rate, but when P_{O2} was doubled again ("1"), the mass began to decrease slowly (EE_{O2} ≈ 2.1 x 10^{-5} Da/O_2 collision). Doubling again, and again ("2" and "3") had no effect on mass loss rate, i.e., EE_{O2} decreased, then at the two highest pressures the mass loss rate increased, such that EE_{O2} was constant at ~7 x 10^{-6} Da/O_2 collision. Thus, increasing P_{O2} by nearly two orders of magnitude did result in a small amount of etching, but with EE_{O2} ~100 times smaller that the initial EE_{O2}.

Fig. S11 summarizes a similar experiment for another graphite NP, with similar results, i.e., initial EE_{O2} near 10^{-3} Da/O_2 collision, fluctuation about that value as the NP lost ~13% of its initial mass, then increased substantially, to well above the initial EE_{O2}, resulting in an additional ~22% decrease in M, followed by abruptly slowing of the rate by more than two orders of magnitude, followed by 6.5 hours of further slow decline in EE_{O2}. It is conceivable that additional fast etching waves might have occurred if more time had been allowed, but in all the examples of graphitic NPs studied here and previously,[5] we have never observed recovery of oxidation reactivity after periods of more than ~2 hours of near-inertness. The unique aspect of both graphite NPs, not seen for NPs of other carbon materials, was a substantial increase in EE_{O2} to well above the initial values, just prior to abrupt decreases by several orders of magnitude.

In all the experiments with black carbon NPs (**Figs. 4-6**, **S10-S11**), reactivity was initially high, even with a period of 1900 K annealing/sublimation, but the NPs all eventually evolved to inertness after long periods of 1500 K O_2 exposure, with oxidative mass losses ranging between ~7 and ~66% of the initial NP masses.

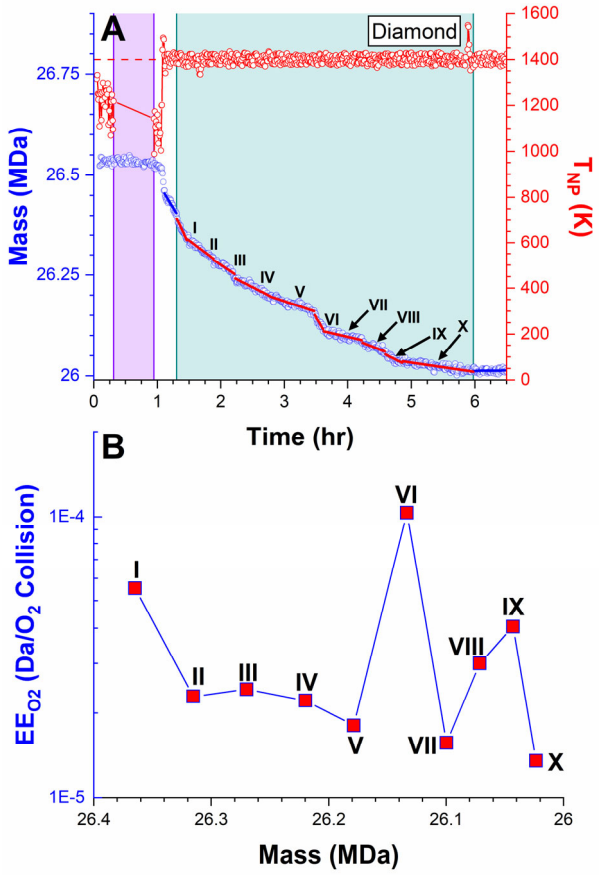

Figure 7. A). A diamond NP at conditions of T_{NP} = 1400 K and P_{O2} = 4.3 x 10^{-5} Torr. B). EE_{O2} vs. mass.

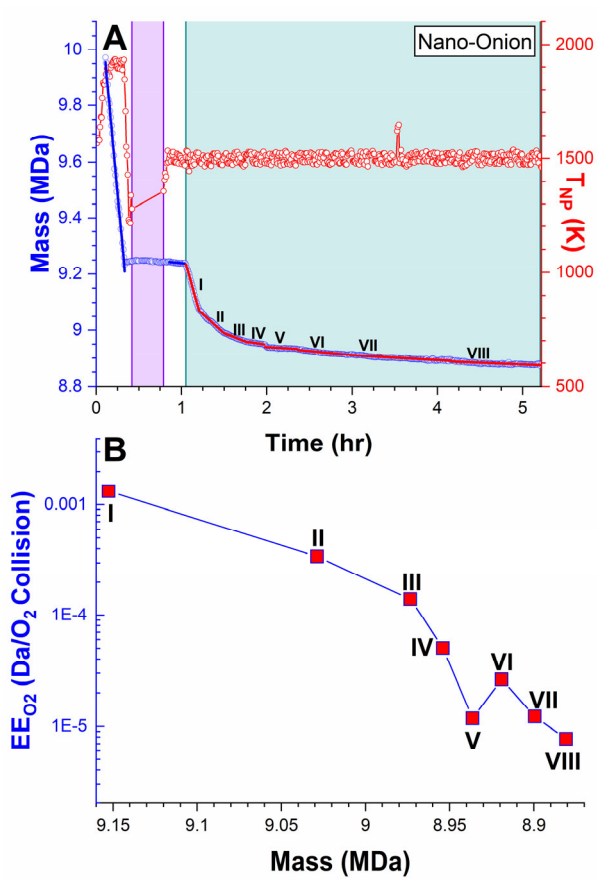

Figure 8. A). A nano-onion NP at constant T_{NP} and P_{O2}. B). EE_{O2} vs. mass shows EE_{O2} rapidly decline.

Comparison of the results in **Figs. 1B**, **2**, and **3**, indicate that diamond NPs can be quite reactive at low T_{NP} (i.e. 1200 K) but are rapidly rendered inert by short periods of 1900 K annealing or short oxidation periods at $T_{NP} \geq$ 1400 K, with loss of only a few percent of $M_{initial}$.

Fig. 7 shows a constant T_{NP}, P_{O2} experiment for a diamond NP, where, in an attempt to preserve the initial high EE_{O2} (**Figs. 2** – **3**), T_{NP} was held at ~1200 K prior to the start of the oxidation period, done at 1400 K to try to slow the evolution. $M_{initial}$ was ~26.5 MDa, probably corresponding to a small aggregate of nano-diamonds. M was stable during the initial ~1200 K period, but as T_{NP} was ramped to 1400 K, M rapidly decreased by ~47 kDa, with $R_{base} \approx$ 0.13 Da/sec/nm^2, stabilizing at ~0.026 Da/sec/nm^2 as soon as T_{NP} reached 1400 K. This behavior is attributed to desorption of some species that were stable at 1200 K, but not at 1400 K. For other carbon NPs experiments, these species would have been lost during the initial 1900 K pre-heating. The nature of the adsorbate is unclear, but C-H and C-O functional groups desorb in this temperature range,[37-38] and the 47 kDa mass loss would be consistent with desorption of a monolayer of H, or loss of a few thousand CO groups from decomposing surface oxygen complexes.

When 4.3 x 10^{-5} Torr of O_2 was added, the mass loss rate increased, but only by ~25%, to ~3.4 x 10^{-2} Da/sec/nm^2, corresponding to an initial EE_{O2} of just ~5.5 x 10^{-5} Da/O_2 collision. The mass loss rate gradually decreased to ~1.3 x 10^{-5} Da/O_2 collision during the ~4.7 hour oxidation period, and when the O_2 flow was stopped, R_{base} also had decreased substantially, as expected because R_{base} in this T_{NP} range is due to reactions with background gases. The initial EE_{O2} was also much lower than the 1500 K initial EE_{O2} values (~10^{-3} Da/O_2 collision) observed for graphite, graphene oxide and carbon black NPs, and the total mass loss (~2%) was much smaller than those seen for the more reactive NPs.

The diamond NP in **Fig. 2** was ~50 times more reactive when initially exposed to O_2 at 1200 K, and remained ~10 times more reactive even after T_{NP} had been ramped to 1400 K. The diamond NP in **Fig. 3** was also substantially (~20x) more reactive at 1200 K, however, its EE_{O2} dropped rapidly even at 1200 K. The obvious conclusion is that the diamond NP in **Fig. 7** had already evolved significantly toward O_2 inertness by the time it was heated to the 1400 K starting point. A similar experiment where oxidation was carried out at 1300 K for another diamond NP is shown in **Fig. S12**, with results similar to those in **Fig. 7**, i.e., significant initial R_{base}, low initial EE_{O2}, slowly declining over time. That NP had been briefly heated above 1500 K just after trapping, thus it also had likely evolved substantially before oxidation was examined. A possible reason why the diamond NPs appear to have evolved at very different rates is discussed below.

As noted above, we previously concluded[5] that graphitic NPs become inert to O_2 at high T_{NP} because they, or at least their surface layers, evolve to have very few under-coordinated surface atoms, and speculated that carbon nano-onion (multi-wall fullerene) structure was most likely. Carbon nano-onions can be made in bulk by annealing nano-diamond[21, 40-44] with structural characterization by TEM. We, therefore, did a number of experiments to characterize the T_{NP} and time dependence of O_2 etching of NPs

from nano-onion feedstock prepared by annealing nano-diamonds in a graphite crucible in an Ar-filled furnace at ~2100 K for 2 hours,[21] giving material with clear nano-onion structure in TEM. **Fig. 8** shows a nano-onion NP oxidation experiment under conditions identical to those used in **Figs. 4**, **5**, **6**, and **S11**. The initial mass was ~9.9 MDa, corresponding to a nominal diameter of ~24.2 nm, assuming a density = 2.21 g/cm^3 [41] for annealed ultra-dispersed diamonds, and it may have been either a single nano-onion or small aggregate.

The NP was held at 1900 K for ~10 minutes, during which time it sublimed at a rate of ~0.5 Da/sec/nm^2, losing ~7% of its initial mass. The 1900 K rate was similar to those seen in **Figs. 1A**, **S2**, **S3**, and **S6B** for graphitic and carbon black NPs (0.29 to 0.44 Da/sec/nm^2). When the T_{NP} was set to 1500 K, R_{base} was 4.7 x 10^{-3} Da/sec/nm^2, also similar to those for other black carbon NPs, and when 4.3 x 10^{-5} Torr of O_2 was added, the initial EE_{O2} (~1.3 x 10^{-3} Da/O_2) was also comparable to the values typical of black carbon NPs. Note, however, that EE_{O2} dropped monotonically, much more quickly, and with much less mass lost, compared to the other black carbon NPs. EE_{O2} for the nano-onion NP slowed by an order of magnitude for less than 3% mass loss, while the equivalent mass losses were 35 to 37% for graphite (**Figs. 6** and **S11**), 15% for graphene oxide (**Fig. 5**), and 5 to 6% for carbon black (**Figs. 4** and **S10**). The total oxidative mass lost as EE_{O2} dropped to just above our sensitivity limit was only ~4%, again much less than for any of the other black carbon materials.

Perfect nano-onions would have no under-coordinated surface sites, and therefore should be inert to O_2 under these conditions (as is HOPG,[11-12] for example), thus the surprise is that the initial EE_{O2} was so large. We conclude that the nano-onion NP initially had either a rather defective surface layer, or had significant surface contamination by non-onion-structured carbon. As this reactive carbon burned away, the NP quickly became inert. For an onion NP of this initial mass, roughly 5.3% of the mass would be in the surface layer, thus the ~4% mass lost as the NP became inert corresponds to only ~0.75 ML.

2.5 – Evolution under Annealing vs. Oxidative Conditions

The experiments above show that all types of carbon NPs evolve under oxidizing conditions, such that EE_{O2} decreases by 2 to 4 orders of magnitude. In contrast, when graphite and graphene NP were heated (to 2100 K) in argon to drive sublimation, the decreases in sublimation rates were much smaller.[4] For example, the average decrease was a factor of 6 at 1800 K and just a factor of 1.6 at 2100 K. Even when an NP was allowed to sublime for >10 hours at 1900 K, losing 12% of its initial mass, $R_{sublimation}$ only slowed by a factor of ~2. These small decreases can be rationalized in terms of modest decreases in the number of under-coordinated surface sites due to the combined effects of annealing and preferential sublimation from the least stable surface sites.

Thus, one question is whether oxidative etching promotes evolution to more stable/less reactive surface structure, or if similar evolution also occurred in the sublimation experiments, but was simply not detected because sublimation is less sensitive to surface structure than oxidation. **Fig. 9** shows three experiments testing this question for graphite, diamond, and nano-onion NPs. The experiments were identical to those in **Figs. 4 – 8**, with the exception that the NPs were held under inert conditions for most of the time, with O_2 only added briefly to probe EE_{O2} at the beginning and end.

Fig. 9A shows the results for a 17.3 MDa (~28.9 nm) graphite NP. As in **Figs. 1A**, **6**, and **S11**, T_{NP} was briefly set to 1900 K to clean the surface, and allow measurement of $R_{sublimation}$, which was ~0.59 Da/sec/nm^2 – comparable to the 1900 K $R_{sublimation}$ values for the graphite NPs in **Figs. 1A**, **6**, and **S11**. T_{NP} was then dropped to

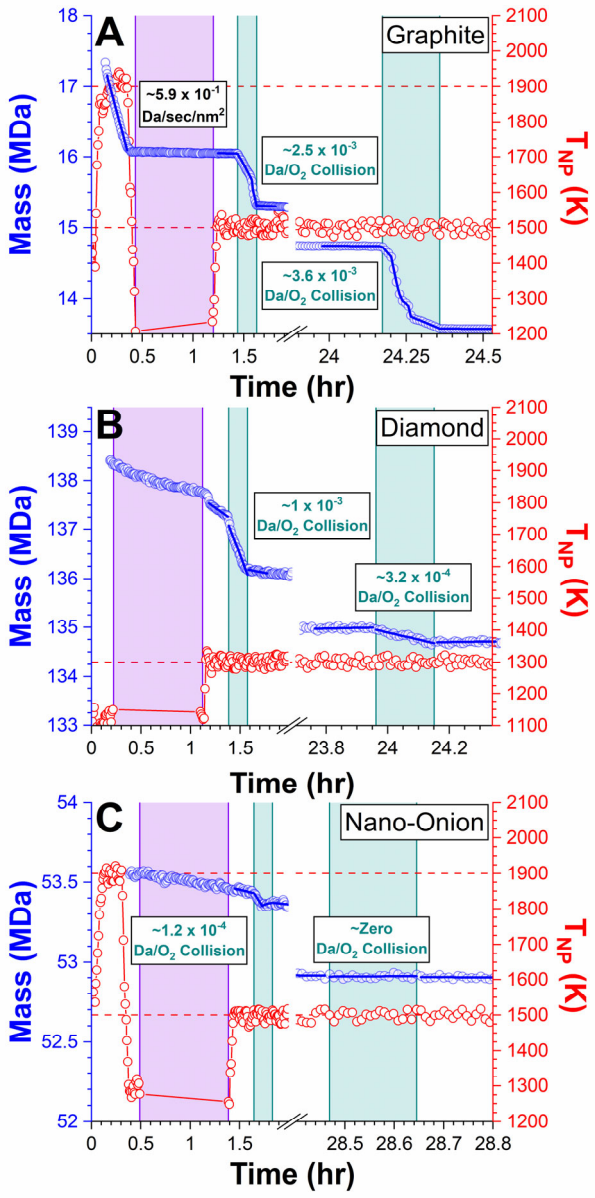

Figure 9. A). A graphite NP is oxidized at 1500 K, annealed for >22 hours, and oxidized again. B). A similar experiment on a diamond NP without pre-heating to 1900 K. C). The same experiment in frame A, but for a nano-onion NP.

1300 K for Q-stepping, and then held at 1500 K for the rest of the experiment. The initial 1500 K R_{base} was also similar to values for the other graphitic NPs, and when 4.3 x 10^{-5} Torr of O_2 was added, EE_{O2} averaged over the 10 minute initial oxidation period was ~2.5 x 10^{-3} Da/O_2 collision, also in the range typical of black carbon NPs. The NP was then held in argon for more than 22 hours (note break and change in time axis), resulting in just ~0.55 MDa (~3%) mass loss, corresponding to average $R_{base} \approx 3 \times 10^{-3}$ Da/sec/nm^2. After the long annealing period, O_2 was re-introduced for a second oxidation period, and while EE_{O2} fluctuated, the average EE_{O2} was ~3.6 x 10^{-3} Da/O_2 collision, i.e., 30% *higher* compared to the initial EE_{O2} value. Clearly, heating in argon did not result in anything close to the three to four orders-of-magnitude decreases in EE_{O2} observed for graphite, graphene,[5] carbon black, and graphene oxide NPs held under oxidizing conditions. The difference is clearly not

simply a result of the relatively small sublimation mass loss, because carbon black NPs become inert for similar mass losses.

Fig. 9B shows an analogous experiment for a diamond NP with initial mass of 138.4 MDa (a large aggregate of nano-diamonds). To minimize structural evolution prior to the initial oxidation, the 1900 K sublimation step was omitted, and the NP was never heated above the 1300 K oxidation temperature, thus this experiment should be directly comparable to the long-term oxidation experiment in **Fig. S12**. As in many of the diamond NP experiments, as T_{NP} was initially ramped from 1150 to 1300 K in argon, there was very fast loss of ~192 kDa of mass, attributed to desorption of adsorbates, then R_{base} stabilized at ~0.053 Da/sec/nm^2. When O_2 was added, the mass loss accelerated and was nearly constant over the 10 minute initial oxidation period, resulting in an initial EE_{O2} (10^{-3} Da/O_2 collision) in the same range as those for other carbon NPs under similar conditions. Note, however, that R_{base} measured just after this oxidation period was much slower than R_{base} just before, indicating that significant evolution occurred in just ~10 minutes of oxidative etching. The NP was then annealed in argon at 1300 K for ~22 hours, during which it lost ~1.1 MDa (~0.8% of $M_{initial}$), and clearly R_{base} continued to slow throughout the annealing period. When the annealed diamond NP was exposed to O_2, EE_{O2} was found to be ~3.2 x 10^{-4} Da/O_2 collision, i.e., the long annealing period resulted in decreased reactivity, but only by a factor of ~3. For comparison, in **Fig. S12**, the final EE_{O2} was only ~2.5 x 10^{-5}, even though the oxidation period was only 10.8 hours long. Both the modest effect of long-term annealing in argon and the large decrease in R_{base} after the initial oxidation period, suggest that oxidizing conditions also promote evolution of diamond NPs toward O_2 inertness, although the results in **Figs. 1B** and **3** show that annealing in the 1900 K range also renders diamond NPs O_2 inert (unlike the graphite, graphene, carbon black, and graphene oxide NPs).

Fig. 9C shows a similar experiment for a nano-onion NP, using the same protocol as **Fig. 9A**. In this case, there was so much thermionic emission during the initial 1900 K pre-heating period that it was impossible to measure the sublimation rate. After Q-stepping and setting T_{NP} to 1500 K, EE_{O2} was measured to be ~1.2 x 10^{-4} Da/O_2 collision, i.e. already an order of magnitude lower than the initial EE_{O2} for the nano-onion NP in **Fig. 8**, or typical initial EE_{O2} values for black carbon NPs. Furthermore, after just ~5 minutes of oxidative etching, having lost ~0.15 MDa (~0.3% of the initial mass), the NP became unreactive toward O_2. We interpret both the low initial EE_{O2} and the rapid transition to inertness during oxidation as indicating that this particular nano-onion NP had very little defective or non-onion carbon on its surface after the 1900 K sublimation period, resulting in low initial EE_{O2} and rapid evolution to inertness as that reactive carbon etched away. The NP was held at 1500 K in argon for a ~26.6 hour annealing period, during which the NP lost ~0.42 MDa (~0.8% of the initial mass), corresponding to $R_{base} \approx$ 7.8 x 10^{-4} Da/sec/nm^2. Given that the NP was already inert before annealing, it is not surprising that it was still inert after annealing (no mass change during the 2nd oxidation period).

3. Discussion

3.1 – Comparison of Initial EE_{O2} and $R_{sublimation}$ for Carbon NPs

Fig. 10 summarizes the initial EE_{O2} values measured for 32 different carbon NPs of the five materials studied, and the 1900 K $R_{sublimation}$ values for 23 carbon NPs. The feedstock materials are indicated by color, and the results are plotted against the NP mass at the time the measurements were made. Except where noted, $R_{sublimation}$ was first measured at 1900 K, then T_{NP} was lowered to 1500 K, and EE_{O2} was measured in 4.3 x 10^{-5} Torr of O_2. Figure numbers next to points indicate data taken from those figures; unlabeled points represent additional NPs studied with the same

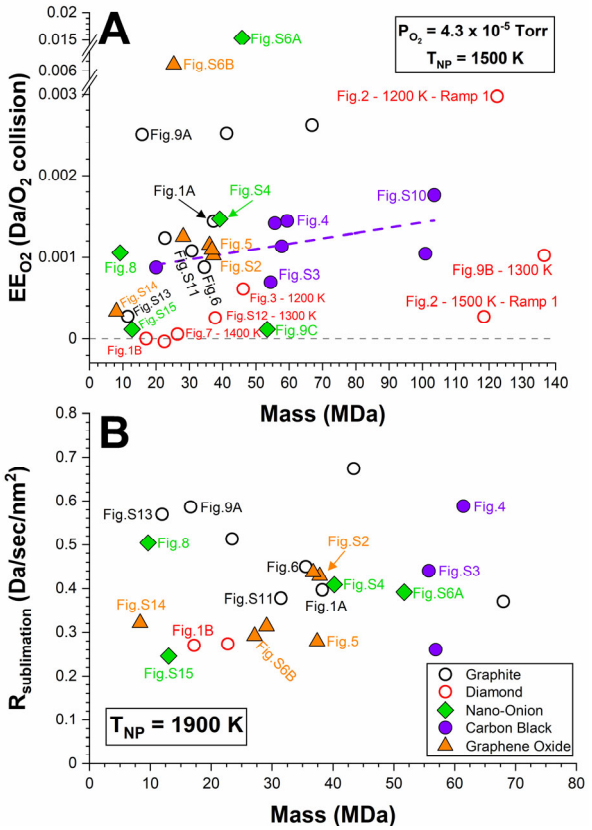

Figure 10: Comparison of the initial oxidation (A) and sublimation (B) kinetics for all carbon NPs studied, showing the large variations between different types of NPs, and the large variation between individual NPs within each type. Values are plotted vs. NP mass to show that, with the exception of carbon black, there are no obvious trends of reactivity vs. mass. A). EE_{O2} vs. mass for 32 carbon NPs, measured at 1500 K unless indicated. A regression line is shown for carbon black, which is the only NP type to show any trend vs. mass. B). $R_{sublimation}$ vs. mass for 23 carbon NPs at T_{NP} = 1900 K.

protocol. Most of the diamond EE_{O2} data were taken at reduced T_{NP} (indicated next to the data points) and without the initial 1900 K sublimation period. The other exception was the carbon black NP from **Fig. S10**, where EE_{O2} was measured at 1500 K, but omitting the 1900 K sublimation period (which, however, had no obvious effect).

One question is whether there might be systematic trends in EE_{O2} vs. NP mass. If reactivity is proportional to the number of reactive sites on the NP surface, then it would depend on the density of reactive surface sites and the NP surface area. The surface area is approximately taken into account in calculating EE_{O2}, assuming spherical NP shape (surface area $\propto M^{2/3}$), and $M^{2/3}$ scaling would still hold for non-spherical NPs if the shapes of different size NPs are similar. In either case, EE_{O2} would tend to be mass-independent, assuming the reactive site density is also size-independent. As noted above, however, many of the larger NPs are almost certainly aggregates of smaller primary particles, and in that scenario, the actual surface areas and the EE_{O2} values should increase with mass.

Carbon black showed the smallest NP-to-NP variation in initial EE_{O2} values, averaging ~1.2 x 10^{-3} Da/O_2 collision, with total variation from the least to most reactive NP being a factor of ~2.5.

This variation is small enough that an increase in EE_{O2} with mass is noticeable, with the values for individual NPs lying within ±40% of the linear regression line plotted in the figure. The small scatter implies that the carbon black NPs must be reasonably homogeneous in the sense that the NP-to-NP variations in shape and reactive site densities are small. This is not the case for any of the other carbon NP types.

For example, the variation in EE_{O2} for the graphite NPs was almost a factor of 10, with average EE_{O2} of ~1.6 x 10^{-3} Da/O_2 collision. Previously reported 1500 K O_2 etching rates for graphitic NPs[5] also give EE_{O2} values in the same broad range. Note, however, that the smallest graphite NP (~11 MDa, raw data in **Fig. S13**) had EE_{O2} about 10 times lower than average, and if this NP is excluded, the EE_{O2} values varied by only a factor of ~three, with average EE_{O2} of ~1.75 x 10^{-3}. NPs with graphitic structures should always be reactive toward O_2. For example, an idealized graphite NP, consisting of a stack of graphene layers, would have unreactive[11-12] basal planes on the top and bottom faces, but the sides would expose the edges of the stacked graphene layers, of which ~50% of the atoms are under-coordinated and reactive toward O_2 in our temperature range.[18] Real graphite NPs should have more sites for a given mass NP due to defects and irregular shapes (i.e. higher surface area). The small graphite NP was, thus, anomalously unreactive, and possible reasons are discussed below.

The average EE_{O2} value for the six graphene oxide NPs was ~1.9 x 10^{-3} Da/O_2 collision, but with large NP-to-NP variation. Four NPs with M near 35 MDa had EE_{O2} values just above 10^{-3} Da/O_2 collision, a ~25 MDa NP was six times more reactive, and as with graphite, the smallest NP (~9 MDa, **Fig. S14**) was an order of magnitude less reactive than average ($EE_{O2} \approx$ 3.3 x 10^{-4} Da/O_2 collision). The graphene oxide feedstock is just a few layers thick, and for the mass range here, such NPs would have basal planes with lateral dimensions in the tens to few hundred nm range, i.e., their actual surface areas would be much larger than is assumed in calculating EE_{O2}. The EE_{O2} values, therefore, significantly overestimate the true EE_{O2} values. Keep in mind however, that O_2 reactivity at perfect basal plane sites is negligible,[11-12] thus reactivity really depends not on the surface area, but rather the number of exposed reactive sites. For graphene oxide NPs the number should be large because the feedstock has a 30% O concentration, and CO loss as the NPs are heated should generate a high density of basal plane defects.

The average diamond NP EE_{O2} was just ~6.5 x 10^{-4} Da/O_2 collision, however, this includes near-zero values for three NPs that were pre-heated before the EE_{O2} measurements, as well as values obtained at T_{NP} < 1500 K for several NPs, ranging up to ~3 x 10^{-3} Da/O_2 collision at 1200 K from **Fig. 2**. Excluding the three pre-heated diamond NPs, the average EE_{O2} is ~1.0 x 10^{-3} Da/O_2 collision – similar to that for the black carbon NPs, albeit measured at lower T_{NP}.

Finally, the nano-onion NPs had an average EE_{O2} of ~3.6 x 10^{-3}, but the individual NP EE_{O2} values varied by over two orders of magnitude, from near zero for two NPs (**Figs. 9C** and **S15**), to one NP with the highest EE_{O2} of the entire set of carbon NPs. As discussed above, we believe that the inherent reactivity of perfect onion surfaces is near zero, and interpret the high reactivity of some nano-onion NPs to be the presence of defective or non-onion-structure carbon on the surface.

As noted, the smallest graphite and graphene oxide NPs were, by large factors, the least reactive NPs for each material. (The other low EE_{O2} cases were diamond or nano-onion NPs which had been pre-treated in ways that we expect to suppress reactivity). Low reactivity could be interpreted to indicate that graphitic NPs with mass in the ~10 MDa range are inherently less reactive than even slightly larger graphitic NPs, however, as discussed above, the graphitic structure should always expose large numbers of reactive edge/defect sites. An alternative explanation might be that these small graphitic NPs, or at least their surface layers, evolved more rapidly during the 1900 K sublimation periods than larger NPs, such that they had already lost most of their under-coordinated surface sites before EE_{O2} was measured. Faster restructuring for small NPs is not unreasonable, because they have a larger fraction of their atoms in surface sites where diffusion/isomerization barriers are lower because coordination is lower.

Fig. 10B plots $R_{sublimation}$ vs. mass for 23 carbon NPs at 1900 K. The main point of interest is that, despite the fact that the EE_{O2} values varied by orders of magnitude, $R_{sublimation}$ varied by only a factor of ~3 over the entire set of NPs, and for each NP type, the individual NPs varied by only ±40% from the average values. Note that the graphene oxide and nano-onion NPs (**Figs. S6A** and **S6B**) that had EE_{O2} 5 to 20 times higher than average for those materials, still had sublimation rates within 15% of the average $R_{sublimation}$ values. These data, therefore support the conclusion noted above (cf. **Fig. 3**) that while both sublimation and oxidation are sensitive to the distribution of NP surface sites,[4-5] O_2 etching chemistry is a far more sensitive probe. In part this undoubtedly reflects the higher T_{NP} range where sublimation occurs, but in addition, it is reasonable to expect that the concerted O_2 dissociation/C-O bond formation required for oxidation should be strongly dependent on the number and type of under-coordinated surface sites.

3.2 – Evolution of EE_{O2} vs. Time and Mass

Because O_2 oxidation is sensitive to the presence of under-coordinated surface sites, it serves as an excellent probe of changes in surface site distributions as NPs evolve under heating and etching conditions. Every type of carbon NP studied was found to evolve at high T_{NP} under oxidizing conditions, eventually becoming inert to O_2, and **Fig. 9** showed that the evolution also can occur under inert conditions, but much more slowly. **Fig. 11** uses EE_{O2} to track the evolution of NPs of all the carbon materials under oxidizing conditions. In **Fig. 11A** EE_{O2} is plotted against $M/M_{initial}$, facilitating comparisons between different size NPs; the absolute masses are given in the figures indicated in the legend. Because evolution is also affected by time, **Fig. 11B** plots EE_{O2} vs. reaction time. As in **Fig. 4**, squares indicate EE_{O2} values averaged over time periods with near-constant rates, and squares with downward arrows indicate periods when EE_{O2} dropped below our sensitivity limit.

There are several obvious points. Apart from the two diamond NPs, the *initial* EE_{O2} values were quite similar for all the NPs, clustering around 10^{-3} Da/O_2 collision. The time and mass dependences of EE_{O2} were quite different for each NP, however, indicating that evolution is strongly affected by the NP structure, which varies for the different feedstock materials, but also from NP-to-NP.

The two graphite NPs had by far the largest mass losses before finally becoming inert and for both, EE_{O2} remained significant for >10 hours, but varied by orders of magnitude during that time. The EE_{O2} values for both initially increased by factors of 2 and 3 during the first ~half hour, then declined slowly for several hours, before increasing to 5 to 20 times the initial EE_{O2} values, resulting in a 2nd wave of fast etching that lasted between 2 and 2.5 hours, and removed an additional ~17 to ~20 % of $M_{initial}$. Both the initial increase in EE_{O2} and the second etching wave with EE_{O2} were well above the initial values and seen only for graphite NPs. For one graphite NP (open black) the second wave ended as EE_{O2} gradually decreased, reaching ~10^{-5} Da/O_2 collision at the 11 hour mark when the experiment was ended. The 2nd wave for the other graphite NP (green) ended when EE_{O2} suddenly dropped by >4 orders of

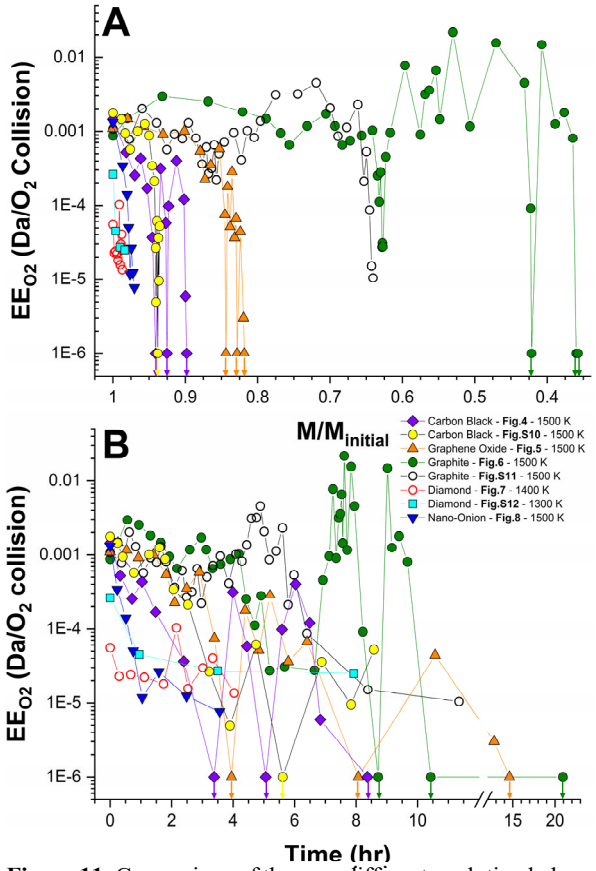

Figure 11: Comparison of the very different evolution behavior of different carbon NPs, using EE_{O2} as a probe. A). EE_{O2} plotted vs. remaining mass fraction, $M/M_{initial}$. B). EE_{O2} plotted vs. time. The figures indicated in the legend show the unaggregated data.

magnitude, then almost immediately rebounded, starting a 3rd oxidation wave that ended at the ~10.5 hour mark when the EE_{O2} dropped below ~10^{-6} Da/O_2 collision and remained negligible for >10 hours, at which point the experiment ended.

Many of the other carbon NPs also etched in multiple waves punctuated by brief periods with near-zero EE_{O2}, however, the EE_{O2} values tended to drop over time, such that the peak EE_{O2} values in succeeding waves remained well below the initial EE_{O2} values. The total mass lost before becoming inert was also much smaller than for graphite, and little mass loss occurred except in the first wave. For example, the initial EE_{O2} values for both carbon black NPs were ~10^{-3} Da/O_2 collision, similar to values for the graphite NPs, but because EE_{O2} decreased during the initial 3 to 4 hour etching wave, only ~6% of $M_{initial}$ was lost. Each carbon black NP also had one or two additional etching waves lasting up to several hours each, however, the rates remained low and there was little additional mass loss. Similarly, the graphene oxide NP also had initial EE_{O2} similar to those for the graphite NPs, and for the first ~2.5 hours it evolved quite similarly to one of the graphite NPs (**Fig. S11**, open black), including a small increase in EE_{O2} at short times, followed by slowly decreasing reactivity. At the ~3.5 hour point, however, the graphene oxide NP rapidly became unreactive, reaching our sensitivity limit at ~4 hours after just ~16% mass loss, and although there were two additional etching waves during the next 11 hours, the EE_{O2} values remained low so that little additional mass was lost.

The diamond NPs behaved differently from the other carbon NPs in two seemingly contradictory ways. On one hand, the diamond initial EE_{O2} values were five to ten times lower than those for the other NPs, but the diamond NP were also the only ones for which EE_{O2} never dropped below 10^{-5} Da/O_2 collision. The low initial reactivity is attributed to these NPs having been pre-heated prior to the start of oxidation, so that they had already partially evolved, and the failure to become completely inert is likely due to the fact that these experiments were done at 100 to 200 K lower T_{NP} than the others, which probably slowed the continued evolution of the NPs. **Figs. 1B, 2** and **3** show that diamond NPs can have EE_{O2} comparable to other carbon NPs, and do become inert if the experiments are run at higher T_{NP}.

Finally, the EE_{O2} for the carbon nano-onion NP, which was initially just above 10^{-3} Da/O_2 collision, similar to the other black carbon NPs, quickly dropped by 2 orders of magnitude as the NP lost ~4% of $M_{initial}$. As already discussed, we believe the initial high reactivity reflects the presence of reactive (non-onion) carbon on the NP surface, with reactivity dropping quickly as this material oxidized away or isomerized to onion structure.

In summary, NPs of all the carbon materials, except diamond, had initial EE_{O2} values of ~10^{-3} Da/O_2 collision, and diamond NPs also had similar initial EE_{O2} values provided that they were never heated above 1200 to 1300 K. O_2 etching requires that O_2 adsorb on the NP surface, which almost certainly implies dissociative adsorption at the high temperatures of our experiments. This creates oxidized surface sites of various structures, which then decay by desorption of CO, CO_2, or O. Minton and co-workers[10] have reported experiments that show primarily CO desorption in the 1200 to 1500 K range, with significant O atom desorption above 1500 K, which would not result in mass loss in our experiments. O_2 is known to have near-zero dissociative sticking probability on perfect graphite basal planes,[11-12] but the edges of graphite basal planes, and basal plane defects are reactive due to the presence of under-coordinated carbon sites. Thus, the similarity in initial EE_{O2} values suggests that all the carbon NP feedstocks have similar initial densities of reactive sites.

3.3 – Structural Evolution of Carbon NPs during Oxidation

To become inert, an NP, or at least its surface layer, must transform to a structure with few under-coordinated sites. The fact that different carbon materials evolve at different rates presumably reflects the differences in the feedstock structure. For example, carbon black NPs become inert after losing only ~10% of their initial mass, and this may reflect the fact that primary carbon black NPs are roughly spherical, lamellar structures of graphene-like platelets,[45] which could form nano-onions by linking the platelets together to form continuous layers. Thus, carbon black NPs would appear to require the least large-scale structural reorganization to "onionize".

In contrast, graphite, in addition to being the most stable form of bulk carbon, has a flat layered structure that would require large-scale reorganization to fully onionize, and these factors presumably account for the observation that the transition to inertness requires long oxidation times with large mass losses. O_2 is known to be unreactive with perfect basal plane sites,[11-12] but is reactive with defects in exposed basal planes,[14, 35] and with the "prismatic" faces of graphite crystallites,[18, 36] i.e., faces that expose the edges of the stacked basal planes. Lateral etching at basal plane defects is substantially faster than etching into the underlying basal plane, and thus tends to form 2D "etch pits" that expand as O_2 etches under-coordinated atoms around the internal perimeter,[13, 15-17, 34] and as the pit expands, the etching rate increases. Thus, etching rates may fluctuate, increasing as pits expand, then decreasing as the basal plane is consumed, exposing the underlying plane, and

this may explain the fluctuations observed during etching of graphitic NPs in which the rate varies substantially as masses equivalent to ~half to a few ML are etched (**Figs. 6**, **9**, **S6B**, **S11**, and previous examples at different T_{NP}[5]).

Because the prismatic faces of graphite are reactive with O_2 in our T_{NP} range, to become inert to O_2 these faces have to reconstruct to eliminate under-coordinated reactive sites. Graphite prismatic edges are known to form "closed-edge" structures, where a graphene sheet can fold over and connect to the edge of a neighboring sheet, forming a bilayer connected by a highly curved, but closed edge (also known as looped or arched edge structures).[46-47] Furthermore, concentric closed/arched edge surfaces can connect together a series of sheets, effectively converting that portion of the prismatic face to a fully coordinated structure.[47] Thus, a possible intermediate step toward encasing graphitic NPs in a fully-coordinated shell might be formation of closed/arched structures. Eventually, such curved sheets might connect completely across the prismatic faces, leaving a fully-coordinated surface.

Fig. 9 shows that evolution of graphite NPs toward inertness is greatly accelerated under O_2 etching conditions, compared to inert conditions at the same T_{NP}. The origin of this effect is not clear, however, for T_{NP} in the 1500 K range, sublimation is negligible and because T_{NP} is only at ~30% of the graphite melting point (4800 K at high pressures)[48] annealing is presumably also slow. Under etching conditions, the rate at which material is removed and the rate at which new under-coordinated sites are exposed by loss of carbon atoms, are relatively fast, with most of the action occurring at the prismatic faces. Thus, etching tends to re-shape the prismatic edges, creating under-coordinated sites that potentially can link together to start the process of creating arched edges. Because etching occurs primarily at under-coordinated sites, once arched structures are formed, they should be less reactive than the surrounding prismatic surface. The waves of etching, separated by periods of low reactivity imply that the graphite NPs can become capped with a fully-coordinated and nearly inert surface layer, but that this layer can be disrupted and etched away, exposing the underlying highly reactive prismatic faces.

For bulk samples of diamond NPs, conversion to nano-onions is often done by high temperature annealing.[21, 40-44] At T > 1000 K, surface reconstructions are known to occur that force carbon atom dimerization.[37-38] The reconstructed diamond surface is thought to contain little to zero hydrogen, and thus promotes graphitization by reducing cleavage energies by ~50%.[1] The other factor is the surface itself, where different planes graphitize at varying rates. In the range of 1400 – 1900 K, the (111) surface is considered the most reactive,[49] due to its buckled hexagons,with dimensions similar to hexagons in graphite (0001).[50] This factor is proposed to promote cleavage and exfoliation of graphite-like layers that encapsulate the diamond NP.

The final interesting point concerns the slow mass losses observed after carbon NPs of all types had become inert to O_2 etching at long times. For example, after the graphene oxide NP in **Fig. 5** finally became inert at ~16 hours, it lost an additional ~90 kDa of mass over the next 6 hours, and the graphite NP in **Fig. 6** lost ~80 kDa in the 11 hours after it finally became inert. These slow mass losses were under oxidizing conditions, but it is not clear they result from O_2 etching, sublimation, or both.

The interesting point is not that the inert NPs continued to lose mass slowly, but rather that they were able to lose thousands of atoms without creating surface defects that restored the NPs' reactivity. Perfect graphite basal planes are inert to O_2,[11-12] but if the surface is sputtered to create defects, O_2 reactions at the defects create etch pits that expand and consume the defective basal plane.[14-15, 17, 51-52] Analogous behavior for the onionized surface layer of an NP would result in an etching wave removing the surface layer. Isomerization within the surface layer allow accommodation of some carbon loss without creating reactive sites, but clearly there there must be a limit. The graphite NP in **Fig. 6** had M =12.42 MDa at the point when it finally became inert. The NP then lost ~6700 atoms (~80 kDa) without regaining reactivity, corresponding to more than 10% of the surface layer for a spherical NP of this mass. Furthermore, when P_{O2} was increased at the end of the oxidation period, an additional ~250 kDa was lost without EE_{O2} ever rising above ~3% of its initial value, i.e., the NP was able to lose mass corresponding to ~half of the surface layer, without triggering fast etching. Finally, in the flash heating experiments (**Figs. 3** and **S9**), even larger mass losses occurred on time scales of a few seconds without restoring reactivity. As outlined in the SI, similar considerations make it unlikely that the "inert" structures formed at long etching times could have spiral layers.

The obvious conclusion is that when a carbon NP finally becomes "permanently" inert, the surface layer must be coupled strongly enough to the underlying NP to allow healing of surface defects by carbon diffusion from underlying layers. Our typical P_{O2} corresponds to ~150 O_2 collisions *per* second *per* nm^2 of surface area (~4 collisions/surface atom/sec) suggesting that inter-layer diffusion need not be very fast.

Furthermore, if inter-layer diffusion is needed to maintain inertness as NPs slowly lose carbon, that might explain why many carbon NPs alternated between periods of inertness and fast etching as they evolved (**Fig.11**). During inert periods, the NPs must have been capped by a fully-coordinated surface layer, but if inter-layer diffusion in *partially* evolved NPs were slow, then carbon loss from the surface layer would eventually overwhelm the defect healing possible from intra-layer processes, triggering a wave of fast etching.

For perfect, defect-free multi-layer nano-onions, one might expect that the stability of the nested shells could be high enough to completely stop carbon atom loss for certain "magic" NP sizes, however, this was never observed. Note, however, that even after etching to the point of O_2-inertness, our NPs were still relatively large, containing >500,000 atoms. For such large onions at high T_{NP}, there must be large ensembles of thermally accessible isomers at high T_{NP}, and enough thermal energy to drive isomerization, thus trapping into a single (or small number of) perfect inert structure(s) would be unlikely.

Carbon NP oxidation has been studied extensively using ensemble methods such as flow tube reactors or flames. These methods have a number of major advantages, such as much higher experimental throughput, the ability to collect product NPs for post-reaction imaging or other analysis, and the ability to measure time scales ranging from hundreds of microseconds to a few seconds. The single NP approach used here is slow and limited, however, it allows several different effects of NP heterogeneity to be observed, that are averaged out in ensemble methods. We can measure the differences in reactivity between different individual NPs, but as illustrated in this study, we can also follow evolution of individual NPs as their etching rates fluctuate dramatically, eventually dropping to near zero. Single NP mass spectrometry, thus, provides a unique tool for examining structural evolution of carbon nanomaterials at high temperatures.

4. Conclusion

Experiments probing O_2 oxidation, sublimation, and annealing kinetics for carbon NPs demonstrated that O_2 etching efficiency is a sensitive probe of NP surface structure, allowing the structural evolution of NPs to be studied in detail. Different types of carbon NPs all have similar initial EE_{O2} values, and all eventually evolve

to become nearly inert to O_2 attack, but the trajectory of the evolution varies substantially between different materials, and from NP-to-NP within each material type.

ASSOCIATED CONTENT

Supporting Information. Additional background information, experimental methods and materials, and supporting figures. This material is available free of charge via the Internet at http://pubs.acs.org."

AUTHOR INFORMATION

Corresponding Author

*Scott L. Anderson – anderson@chem.utah.edu

Author Contributions

All authors have given approval to the final version of the manuscript.

Funding Sources

Dept. of Energy, Office of Science, Gas Phase Chemical Physics program, grant DE-SC0018049

ACKNOWLEDGMENT

The nIR spectrograph was purchased with funds from the Albaugh Scientific Equipment Endowment of the College of Science, University of Utah. This material is based upon work supported by the U.S. Department of Energy, Office of Science, Office of Basic Energy Sciences, under Award Number DE-SC- 0018049.

ABBREVIATIONS

NP, nanoparticle; T_{NP} nanoparticle temperature; P_{O2}, oxygen partial pressure; EE_{O2}, O_2 etching efficiency.

REFERENCES

1. Kuznetsov, V. L.; Butenko, Y. V., 13 - Diamond Phase Transitions at Nanoscale. In *Ultrananocrystalline Diamond*, Shenderova, O. A.; Gruen, D. M., Eds. William Andrew Publishing: Norwich, NY, 2006; pp 405-475.
2. Mykhailiv, O.; Zubyk, H.; Plonska-Brzezinska, M. E., Carbon nano-onions: Unique carbon nanostructures with fascinating properties and their potential applications. *Inorganica Chimica Acta* **2017,** *468*, 49-66.
3. Nienow, A. M.; Roberts, J. T.; Zachariah, M. R., Surface Chemistry of Nanometer-Sized Aerosol Particles: Reactions of Molecular Oxygen with 30 nm Soot Particles as a Function of Oxygen Partial Pressure. *J. Phys. Chem. B* **2005,** *109* (12), 5561-5568.
4. Long, B. A.; Lau, C. Y.; Rodriguez, D. J.; Tang, S. A.; Anderson, S. L., Sublimation Kinetics for Individual Graphite and Graphene Nano-particles (NPs): NP-to-NP Variations and Evolving Structure-Kinetics and Structure-Emissivity Relationships. *J. Am. Chem. Soc.* **2020,** *142* (33), 14090-14101.
5. Rodriguez, D. J.; Lau, C. Y.; Long, B. A.; Tang, S. A.; Friese, A. M.; Anderson, S. L., O_2-oxidation of individual graphite and graphene nanoparticles in the 1200–2200 K range: Particle-to-particle variations and the evolution of the reaction rates and optical properties. *Carbon* **2021,** *173*, 286-300.
6. Marshall, A. L.; Norton, F. J., Carbon Vapor Pressure and Heat of Vaporization. *J. Am. Chem. Soc.* **1950,** *72* (5), 2166-2171.
7. Clarke, J. T.; Fox, B. R., Rate and Heat of Vaporization of Graphite above 3000°K. *J. Chem. Phys.* **1969,** *51* (8), 3231-3240.
8. Tsai, C. C.; Gabriel, T. A.; Haines, J. R.; Rasmussen, D. A., Graphite Sublimation Tests For Target Development For The Muon Collider/Neutrino Factory *IEEE Symp. Fusion Eng.* **2006,** *21*, 377-379.
9. Murray, V. J.; Marshall, B. C.; Woodburn, P. J.; Minton, T. K., Inelastic and Reactive Scattering Dynamics of Hyperthermal O and O_2 on Hot Vitreous Carbon Surfaces. *J. Phys. Chem. C* **2015,** *119*, 14780-14796.
10. Murray, V. J.; Smoll, E. J.; Minton, T. K., Dynamics of Graphite Oxidation at High Temperature. *J. Phys. Chem. C* **2018,** *122* (12), 6602-6617.
11. Olander, D. R.; Siekhaus, W.; Jones, R.; Schwarz, J. A., Reactions of Modulated Molecular Beams with Pyrolytic Graphite. I. Oxidation of the Basal Plane. *J. Chem. Phys.* **1972,** *57* (1), 408-420.
12. Barber, M.; Evans, E. L.; Thomas, J. M., Oxygen chemisorption on the basal faces of graphite: an XPS study. *Chemical Physics Letters* **1973,** *18* (3), 423-425.
13. Stevens, F.; Kolodny, L. A.; Beebe, T. P., Jr., Kinetics of Graphite Oxidation: Monolayer and Multilayer Etch Pits in HOPG Studied by STM. *J. Phys. Chem. B* **1998,** *102* (52), 10799-10804.
14. Lee, S. M.; Lee, Y. H.; Hwang, Y. G.; Hahn, J. R.; Kang, H., Defect-Induced Oxidation of Graphite. *Physical Review Letters* **1999,** *82* (1), 217-220.
15. Hahn, J. R.; Kang, H., Conversion efficiency of graphite atomic-scale defects to etched pits in thermal oxidation reaction. *J. Vac. Sci. Technol., A* **1999,** *17* (4, Pt. 1), 1606-1609.
16. Hahn, J. R., Kinetic study of graphite oxidation along two lattice directions. *Carbon* **2005,** *43* (7), 1506-1511.
17. Edel, R.; Grabnic, T.; Wiggins, B.; Sibener, S. J., Atomically-Resolved Oxidative Erosion and Ablation of Basal Plane HOPG Graphite Using Supersonic Beams of O2 with Scanning Tunneling Microscopy Visualization. *The Journal of Physical Chemistry C* **2018,** *122* (26), 14706-14713.
18. Olander, D. R.; Jones, R. H.; Schwarz, J. A.; Siekhaus, W. J., Reactions of Modulated Molecular Beams with Pyrolytic Graphite. II Oxidation of the Prism Plane. *The Journal of Chemical Physics* **1972,** *57* (1), 421-433.
19. Walls, J. R.; Strickland-Constable, R. F., Oxidation of Carbon between 1000 - 2400 C. *Carbon* **1964,** *1*, 333-338.
20. Rosner, D. E.; Allendorf, H. D., Comparative studies of the attack of pyrolytic and isotropic graphite by atomic and molecular oxygen at high temperatures. *AIAA Journal* **1968,** *6* (4), 650-654.
21. Kovalenko, I.; Bucknall, D. G.; Yushin, G., Detonation Nanodiamond and Onion-Like-Carbon-Embedded Polyaniline for Supercapacitors. *Advanced Functional Materials* **2010,** *20* (22), 3979-3986.
22. Howder, C. R.; Bell, D. M.; Anderson, S. L., Optically Detected, Single Nanoparticle Mass Spectrometer With Pre-Filtered Electrospray Nanoparticle Source. *Rev. Sci. Instrum.* **2014,** *85*, 014104 -014110.
23. Long, B. A.; Rodriguez, D. J.; Lau, C. Y.; Anderson, S. L., Thermal emission spectroscopy for single nanoparticle temperature measurement: optical system design and calibration. *Appl. Opt.* **2019,** *58* (3), 642-649.
24. Long, B. A.; Rodriguez, D. J.; Lau, C. Y.; Schultz, M.; Anderson, S. L., Thermal Emission Spectroscopy of Single, Isolated Carbon Nanoparticles: Effects of Particle Size, Material, Charge, Excitation Wavelength, and Thermal History. *J. Phys. Chem. C* **2020,** *124*, 1704-1716.
25. Bacon, G. E., The interlayer spacing of graphite. *Acta Crystallogr. A* **1951,** *4* (6), 558-561.
26. Tremblay, G.; Vastola, F. J.; Walker, P. L., Jr., Characterization of Graphite Surface Complexes by Temperature-Programmed Desorption. *Extended Abstracts - Bienneial Conf. on Carbon* **1975,** *12*, 177-178.
27. Marchon, B.; Carrazza, J.; Heinemann, H.; Somorjai, G. A., TPD and XPS studies of O2, CO2, and H2O adsorption on clean polycrystalline graphite. *Carbon* **1988,** *26* (4), 507-514.
28. Pan, Z.; Yang, R. T., Strongly Bonded Oxygen in Graphite: Detection by High-Temperature TPD and Characterization *Ind. Eng. Chem. Res.* **1992,** *31*, 2675-2680.
29. Olszak-Humienik, M., On the thermal stability of some ammonium salts. *Thermochim. Acta* **2001,** *378* (1), 107-112.
30. Chupka, W. A.; Inghram, M. G., Molecular Species Evaporating from a Carbon Surface. *J. Chem. Phys.* **1953,** *21* (7), 1313-1313.
31. Drowart, J.; Burns, R. P.; DeMaria, G.; Inghram, M. G., Mass Spectrometric Study of Carbon Vapor. *J. Chem. Phys.* **1959,** *31* (4), 1131-1132.
32. Steele, W. C.; Bourgelas, F. N. *Studies of Graphite Vaporization Using a Modulated Beam Mass Spectrometer, Technical report AFML-TR-72-222, AVSD-0048-73-CR*; Air Force Materials Laboratory, Air Force Systems Command: Wright-Patterson Air Force Base, Ohio, 1972.
33. Pflieger, R.; Sheindlin, M.; Colle, J.-Y., Advances in the mass spectrometric study of the laser vaporization of graphite. *J. Appl. Phys.* **2008,** *104* (5), 054902.
34. Chang, H.; Bard, A. J., Formation of monolayer pits of controlled nanometer size on highly oriented pyrolytic graphite by gasification reactions as studied by scanning tunneling microscopy. *J. Am. Chem. Soc.* **1990,** *112* (11), 4598-9.
35. Nowakowski, M. J.; Vohs, J. M.; Bonnell, D. A., Surface reactivity of oxygen on cleaved and sputtered graphite. *Surf. Sci.* **1992,** *271* (3), L351-L356.
36. Radovic, L. R., Active Sites in Graphene and the Mechanism of CO2 Formation in Carbon Oxidation. *Journal of the American Chemical Society* **2009,** *131* (47), 17166-17175.
37. Hamza, A. V.; Kubiak, G. D.; Stulen, R. H., The role of hydrogen on the diamond C(111)−(2 × 1) reconstruction. *Surface Science* **1988,** *206* (1), L833-L844.
38. Hamza, A. V.; Kubiak, G. D.; Stulen, R. H., Hydrogen chemisorption and the structure of the diamond C(100)-(2 × 1) surface. *Surface Science* **1990,** *237* (1), 35-52.
39. Rossman, R. P.; Smith, W. R., Density of Carbon Black by Helium Displacement. *Ind. Eng. Chem. Res.* **1943,** *35* (9), 972-976.
40. Kuznetsov, V. L.; Chuvilin, A. L.; Butenko, Y. V.; Mal'kov, I. Y.; Titov, V. M., Onion-like carbon from ultra-disperse diamond. *Chemical Physics Letters* **1994,** *222* (4), 343-348.
41. Butenko, Y. V.; Kuznetsov, V.; Chuvilin, A.; Kolomiichuk, V.; Stankus, S.; Khairulin, R.; Segall, B., Kinetics of the graphitization of dispersed diamonds at "low" temperatures. *Journal of Applied Physics* **2000,** *88* (7), 4380-4388.
42. Butenko, Y. V.; Krishnamurthy, S.; Chakraborty, A.; Kuznetsov, V.; Dhanak, V.; Hunt, M.; Šiller, L., Photoemission study of onionlike carbons produced by annealing nanodiamonds. *Physical review B* **2005,** *71* (7), 075420.

43. Zou, Q.; Li, Y.; Lv, B.; Wang, M.; Zou, L.; Zhao, Y., Transformation of onion-like carbon from nanodiamond by annealing. *Inorganic Materials* **2010,** *46* (2), 127-131.
44. Bogdanov, K.; Fedorov, A.; Osipov, V.; Enoki, T.; Takai, K.; Hayashi, T.; Ermakov, V.; Moshkalev, S.; Baranov, A., Annealing-induced structural changes of carbon onions: High-resolution transmission electron microscopy and Raman studies. *Carbon* **2014,** *73*, 78-86.
45. Fan, C.; Liu, Y.; Zhu, J.; Wang, L.; Chen, X.; Zhang, S.; Song, H.; Jia, D., Understanding the structural transformation of carbon black from solid spheres to hollow polyhedra during high temperature treatment. *RSC advances* **2019,** *9* (51), 29779-29783.
46. Rotkin, S. V.; Gogotsi, Y., Analysis of non-planar graphitic structures: from arched edge planes of graphite crystals to nanotubes. *Materials Research Innovations* **2002,** *5* (5), 191-200.
47. Posligua, V.; Bustamante, J.; Zambrano, C. H.; Harris, P. J.; Grau-Crespo, R., The closed-edge structure of graphite and the effect of electrostatic charging. *RSC Advances* **2020,** *10* (13), 7994-8001.
48. Savvatimskiy, A. I., Measurements of the melting point of graphite and the properties of liquid carbon (a review for 1963–2003). *Carbon* **2005,** *43* (6), 1115-1142.
49. Evans, T., Changes produced by high temperature treatment of diamond. *The properties of diamond* **1979**, 403-425.
50. Kuznetsov, V. L.; Zilberberg, I. L.; Butenko, Y. V.; Chuvilin, A. L.; Segall, B., Theoretical study of the formation of closed curved graphite-like structures during annealing of diamond surface. *Journal of Applied Physics* **1999,** *86* (2), 863-870.
51. Hahn, J. R.; Kang, H.; Lee, S. M.; Lee, Y. H., Mechanistic Study of Defect-Induced Oxidation of Graphite. *J. Phys. Chem. B* **1999,** *103* (45), 9944-9951.
52. Hahn, J. R.; Kang, H., Spatial distribution of defects generated by hyperthermal Ar+ impact onto graphite. *Surf. Sci.* **2000,** *446* (1-2), L77-L82.

Insert Table of Contents artwork here